

Viral dynamics *in vivo*: Limitations on estimates of intracellular delay and virus decay

(human immunodeficiency virus/hepatitis B virus/reverse transcriptase inhibitor/protease inhibitor/mathematical model)

ANDREAS V. M. HERZ, SEBASTIAN BONHOEFFER, ROY M. ANDERSON, ROBERT M. MAY, AND MARTIN A. NOWAK*

Department of Zoology, University of Oxford, South Parks Road, OX1 3PS, Oxford, United Kingdom

Contributed by Robert M. May, March 14, 1996

ABSTRACT Anti-viral drug treatment of human immunodeficiency virus type 1 (HIV-1) and hepatitis B virus (HBV) infections causes rapid reduction in plasma virus load. Viral decline occurs in several phases and provides information on important kinetic constants of virus replication *in vivo* and pharmacodynamical properties. We develop a mathematical model that takes into account the intracellular phase of the viral life-cycle, defined as the time between infection of a cell and production of new virus particles. We derive analytic solutions for the dynamics following treatment with reverse transcriptase inhibitors, protease inhibitors, or a combination of both. For HIV-1, our results show that the phase of rapid decay in plasma virus (days 2–7) allows precise estimates for the turnover rate of productively infected cells. The initial quasi-stationary phase (days 0–1) and the transition phase (days 1–2) are explained by the combined effects of pharmacological and intracellular delays, the clearance of free virus particles, and the decay of infected cells. Reliable estimates of the first three quantities are not possible from data on virus load only; such estimates require additional measurements. In contrast with HIV-1, for HBV our model predicts that frequent early sampling of plasma virus will lead to reliable estimates of the free virus half-life and the pharmacological properties of the administered drug. On the other hand, for HBV the half-life of infected cells cannot be estimated from plasma virus decay.

Clinical studies of drug therapy in patients infected with the human immunodeficiency virus type 1 (HIV-1) (1–4) or the hepatitis B virus (HBV) (5) provide for the possibility of estimating important kinetic constants of virus replication *in vivo*.

In HIV-1 infection, treatment with reverse transcriptase or protease inhibitors results in a decline of free virus in several distinct phases (see Fig. 1). Initially, the plasma virus load remains at approximately pretreatment levels which are quasi-stationary on the time scale of weeks in the asymptomatic stage of the infection. This “shoulder” is followed by a rapid and approximately exponential decline of plasma virus and an increase in CD4 cell counts. The reduction of virus load is caused by two factors: decay of productively infected cells and clearance of free virus particles. Finally, the decline flattens out and virus levels may even rise again. This is a consequence of some combination of the following factors: (i) the drug not being 100% effective, (ii) reservoirs of long-lived cells that continuously produce virus particles, and (iii) the emergence of resistant virus (1, 6–8).

If the clearance rate of free virus particles is significantly faster than the decay rate of productively infected cells, the slope of the exponential decline provides an estimate of the turnover rate of productively infected cells. Neglecting intracellular delays, the length and shape of the shoulder then reflect the turnover rate of free plasma virus (1, 4). Within this

modeling approach, the half-life of productively infected cells was found to be around 2 days (1, 2, 4). An accurate estimate of the half-life of free virions was not possible because in the initial studies sampling was not frequent enough in the early stages of therapy, but 1.5 days was estimated as an upper bound for the half-life of free virus (1).

Other parameters of HIV dynamics have also been estimated. The initial increase in the CD4 cell count was found to be about 7% per day (1, 2). Judging from the rise of drug-resistant virus in infected peripheral blood mononuclear cells (PBMC), the half-life of defectively infected PBMC was calculated to lie between 50 and 100 days (1). These data also suggest that the overwhelming majority of infected PBMC harbors defective provirus.

Recently, Perelson *et al.* (9) obtained frequent sequential measurements of plasma virus in patients treated with protease inhibitor. Virus load was determined every 2 h until the sixth hour, then every 6 h until day 2, and then every day until day 7. Perelson *et al.* (9) developed a mathematical model for protease inhibitors and fitted theoretically predicted curves of plasma virus decline to the empirical data. They estimated the half-life of productively infected cells to be around 1.6 days and the half-life of plasma virus around 6 h. Using a second and different heuristic model, Perelson *et al.* (9) argued that the intracellular phase of the HIV-1 life cycle is given by the length of the initial shoulder of plasma virus load, minus the sum of pharmacological delay and average life span of plasma virus. In this way they obtained an average of about 0.9 days for the intracellular phase.

Here we develop a new model that provides a single consistent description of short-time HIV dynamics including the effect of intracellular delay. We derive an analytic solution for virus decline and observe that the half-life of infected cells can be calculated with reasonable accuracy from clinical data. The remaining parameters have to be estimated from the length and shape of the initial shoulder. Our analysis indicates that the shoulder is determined by a complicated combination of pharmacological and intracellular delays, the decay of infected cells, and the clearance of free virus particles. The model therefore suggests that, apart from the half-life of infected cells, precise parameter estimates are not possible based on current data.

Description of the Model

Basic models of viral dynamics contain three variables, which are functions of time t : the populations of uninfected cells, $x(t)$, infected cells that produce virus, $y(t)$, and plasma virus, $v(t)$. In a first approximation to the true dynamics, a constant influx λ and death rate d are usually assumed for the uninfected cells. (This is certainly oversimplified, but as will be shown in the next section, more realistic representations of the dynamics of

The publication costs of this article were defrayed in part by page charge payment. This article must therefore be hereby marked “advertisement” in accordance with 18 U.S.C. §1734 solely to indicate this fact.

Abbreviations: HIV, human immunodeficiency virus; HBV, hepatitis B virus.

*To whom reprint requests should be addressed.

uninfected cells do not affect the main conclusions of the present paper.) Uninfected cells and free virus produce uninfected cells at rate $\beta(t)x(t)v(t)$. Infected cells produce free virus particles at rate $k(t)$ and die at rate a . Free virus particles are cleared at rate u . To describe the effects of various drug therapies, the parameters $\beta(t)$ and $k(t)$ are time-dependent, as specified in detail later on. With these assumptions we get

$$dx(t)/dt = \lambda - dx(t) - \beta(t)x(t)v(t), \quad [1]$$

$$dy(t)/dt = \beta(t)x(t)v(t) - ay(t), \quad [2]$$

$$dv(t)/dt = k(t)y(t) - uv(t). \quad [3]$$

This system of differential equations has previously been used to quantify virus dynamics (1, 2, 4, 5). The model does not contain an intracellular time delay between infection of a cell and production of new virus particles. For many aspects of viral dynamics such a delay can be neglected, but as we show in this paper, the intracellular delay is of crucial importance if the model is used to determine the half-life of free virus.

To incorporate the intracellular phase of the virus life-cycle, we assume that virus production lags by a delay τ behind the infection of a cell. This implies that recruitment of virus-producing cells at time t is not given by the density $\beta(t)x(t)v(t)$ of newly infected cells as in Eq. 2, but rather by the density of cells that were newly infected at time $t - \tau$ and are still alive at time t . If we assume a constant death rate \bar{a} for infected but not yet virus-producing cells, the probability of surviving from time $t - \tau$ to time t is just $e^{-\bar{a}\tau}$. [More generally, the survival probability is given by some nonincreasing function $f(\tau)$ with $0 \leq f(\tau) \leq 1$.] Thus the refined model can be written as

$$dx(t)/dt = \lambda - dx(t) - \beta(t)x(t)v(t) \quad [4]$$

$$dy(t)/dt = \beta(t - \tau)x(t - \tau)v(t - \tau)e^{-\bar{a}\tau} - ay(t) \quad [5]$$

$$dv(t)/dt = k(t)y(t) - uv(t). \quad [6]$$

The x and v equations have remained the same, whereas the y equation has become a "delay-differential equation:" the change of the dynamical variable y at time t depends on terms evaluated at the *earlier* time $t - \tau$.

In general, solutions of this type of equation are difficult to find in closed form. However, in the specific problem in question, the populations of uninfected cells, infected virus-producing cells, and free virus are at a steady-state level before treatment sets in. This situation facilitates the mathematical analysis and enables us to derive simple analytical solutions, as will be shown in the next sections. The nontrivial steady state of Eqs. 4–6 is given by

$$x_0 = \frac{au}{\beta k} e^{\bar{a}\tau}, y_0 = \frac{\lambda}{a} e^{-\bar{a}\tau} - \frac{du}{\beta k}, \quad [7]$$

$$\text{and } v_0 = ky_0/u$$

where β and k are constant pretreatment rates.

Reverse Transcriptase Inhibitors

In HIV-1, reverse transcriptase inhibitors block the infection of uninfected cells. In the model this means that $\beta(t)$ is strongly reduced once treatment sets in at time $t = 0$. For simplicity, we assume that the drug has 100% effectiveness—i.e., $\beta(t) = 0$ for $t > 0$. Thus Eq. 4 is modified to

$$dx(t)/dt = \lambda - dx(t) \quad \text{for } t > 0. \quad [8]$$

For $0 < t \leq \tau$, cells that are virus producing at time t were infected at time $t - \tau \leq 0$; that is, before the drug was administered. Thus for these times, the right-hand side of Eq.

5 is given by the pretreatment equilibrium values (Eq. 7) of x and v —and vanishes. For times larger than τ , newly recruited cells would have been infected at time $t - \tau > 0$. However, these infections are blocked by the drug. We therefore obtain

$$dy(t)/dt = \begin{cases} 0 & \text{for } 0 < t \leq \tau, \\ -ay(t) & \text{for } t > \tau. \end{cases} \quad [9]$$

The dynamics of the free virus, given by Eq. 6, are not changed. Inspection of Eqs. 6, 8, and 9 reveals two important facts. (i) Both y and v remain at their steady states until $t = \tau$. (ii) The time-course of uninfected cells x does *not* influence the dynamics of infected cells and free virus for $t > 0$. This implies that possible refinements of Eq. 4 have no effect on $y(t)$ and $x(t)$ —apart from different pretreatment equilibrium values.

Solving Eqs. 6 and 9 with the initial conditions $y(0) = y_0$ and $v(0) = v_0$, one obtains $v(t) = v_0$ for $0 < t \leq \tau$ and

$$v(t) = \frac{v_0}{a - u} [ae^{-u(t-\tau)} - ue^{-a(t-\tau)}] \quad [10]$$

for $t > \tau$. The result shows that a finite time lag between infection of a cell and emission of viral particles is reflected by an equal delay in the resulting time evolution of the abundances of infected cells and free virus. Note that Eq. 10 is symmetric in the parameters a and u so that, in the absence of additional information, a treatment with reverse transcriptase inhibitors cannot be used to distinguish between u and a . In practice, this symmetry is not problematic because independent measurements of the decay of plasma infectivity (9) give a rough estimate for u , showing that $u > a$. In the limit $\tau \rightarrow 0$, the solutions derived in refs. 1 and 4 are recovered.

Protease Inhibitors and Combined Drug Treatment

Protease inhibitors of HIV block the production of new infectious virus v_I from already infected cells. Only noninfectious virus is generated. Previously released infectious virus decays, but continues to infect cells (9, 10).

Within the present framework, Eq. 6 thus still describes the dynamics of the total free virus. Infectious virus v_I , however, is not produced for $t > 0$ and decays according to $dv_I(t)/dt = -uv_I(t)$. Eqs. 4 and 5 remain valid if one replaces v by v_I .

As in the previous case of a treatment based on reverse transcriptase inhibitors, infected cells and total virus load are again not affected for times smaller than the time lag τ . However, the overall situation is more complex in that the dynamics of infected cells and free virus is *not* decoupled from the time-evolution of uninfected cells. This makes it impossible to write down an analytical solution in closed form. As in ref. 9, we therefore switch to a reduced description and assume that the uninfected cell population stays constant, $x(t) = x_0$, for the time scale under consideration.

For $x(t) = x_0$ and exponentially declining $v_I(t)$, Eq. 5 is solved by

$$y(t) = \frac{y_0}{a - u} [ae^{-u(t-\tau)} - ue^{-a(t-\tau)}] \quad [11]$$

for $t > \tau$, the same functional expression as that of $v(t)$ in a treatment with reverse transcriptase inhibitors (Eq. 10). From Eq. 6, the time-evolution of free virus is then given by $v(t) = v_0$ for $0 < t \leq \tau$ and

$$v(t) = v_0 e^{-u(t-\tau)} + \frac{uv_0}{a - u} \left\{ \frac{u}{a - u} [e^{-a(t-\tau)} - e^{-u(t-\tau)}] + a(t - \tau)e^{-u(t-\tau)} \right\} \quad [12]$$

for $t > \tau$. Without intracellular delay ($\tau = 0$), Eq. 12 reduces to the solution given by Perelson *et al.* (9).

For realistic parameter values, computer simulations underline the validity of the assumption $x(t) = x_0$. Numerical solutions of the full model lag by 1–2 h behind solutions of the reduced model but are otherwise almost equivalent. In particular, the reduced description (Eq. 12) represents an excellent approximation to the full model if the turnover rate of free virus is high (see also Eqs. 4–6).

If protease inhibitors and reverse transcriptase inhibitors are administered simultaneously, the population of infected cells changes according to Eq. 9. Since the time evolution of the total virus load is still given by Eq. 6, the time course of free virus is the same as that if only a reverse transcriptase inhibitor had been administered. In other words, the additional use of a protease inhibitor has no effect on short-term changes in the total virus load if very potent reverse transcriptase inhibitors are administered. However, the combined drug treatment may delay the long-term evolution of drug resistant strains of the virus.

Pharmacological Delay

After application of any anti-viral drug, there is a short delay in the pharmacological effect due to the time required for drug absorption, distribution, and penetration into target cells. The simplest assumption is that drug effectiveness rises with a step-like characteristic from 0 to 100% after some fixed pharmacological delay τ_{pharm} . Thus, if Eq. 10 is used to fit clinical data, τ has to be replaced by $\tau \rightarrow \tau_{\text{pharm}} + \tau$. This implies that the intracellular delay itself cannot be determined from data on plasma virus decline without an independent measurement of the pharmacological delay.

More realistic pharmacodynamics, such as first-order kinetics for drug absorption in the gut and blood plasma, translate into a gradual increase of the drug concentration in the blood, and consequently, a gradual increase of the drug effectiveness. For the virus dynamics, this leads to an intricate interplay between pharmacological effects, intracellular delays, the decay of infected cells, and the clearance of free virus particles. In general, the dynamical equations can no longer be solved analytically, but numerical simulations show that, as expected, the transient phase becomes smoother. The same is true if one assumes that virus production sets in gradually after the infection (B. Sulzer, A. U. Neumann, and A. S. Perelson, personal communication).

Analysis of Clinical Data

Fig. 1 summarizes the results of clinical studies (1, 2, 4, 9) in a schematic illustration of the different phases of viral decline following drug treatment *in vivo*. The present model provides a simple and consistent explanation of these data, as shown in Figs. 2 and 3.

Fig. 2 compares the model predictions of plasma virus decline for reverse transcriptase (Eq. 10) and protease (Eq. 12) inhibitors. Since reverse transcriptase inhibitors completely block infection of new cells in our model, the plasma virus begins to decline immediately after the pharmacological and intracellular delay times. The initial decline of plasma virus in the protease inhibitor model is slower because infectious virus that was produced before the start of treatment continues to infect cells. The two models approach each other if the turnover rate of free virus is high.

Differences in plasma virus decay for fixed half-life of infected cells but different viral clearance rates are shown in Fig. 3a for protease inhibitors. Intracellular delays were chosen such that the long-term decline is identical in all cases (see figure legend). The curves differ mostly at the end of the shoulder phase, but even for strongly varying parameters the differences are small. A large viral clearance rate u leads to a

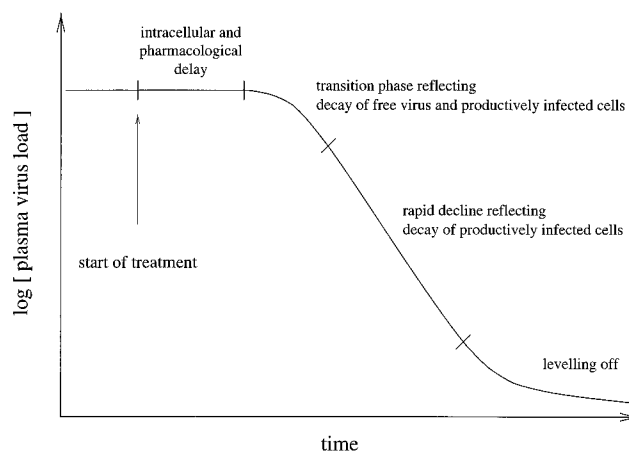


FIG. 1. Schematic illustration of the different phases of plasma virus decline following drug treatment. In the initial phase, the plasma virus load stays constant. The duration of this phase is the sum of the pharmacological delay, defined as the time span the drug needs to reach an effective concentration, and the intracellular delay, defined as the time between infection of a cell and production of new virus particles. The stationary phase is followed by a smooth transition to an approximately exponential decline that mainly reflects the decay of productively infected cells. Finally this decline levels off because of nonoptimal drug effectiveness, reservoirs of virus-producing cells that are not affected by the drug, or the emergence of resistant virus. The length and smoothness of the transition phase is determined by a combination of the half-lives of free virus and infected cells.

sharp edge of the shoulder; a small u leads to a smooth curve. In the examples of Fig. 3A, viral half-lives range from 1.8 to 8.3 h, delays from 2 to 24 h, and yet the virus decay curves remain within a 10% band around the mean solution which is well below present measurement error.

The nearly exponential decline of plasma virus in clinical data can last for up to a week and provides enough information to determine the half-life of infected cells with fair accuracy (1, 2, 9). The reliability of these measurements is also evident from Fig. 3B where solutions with identical intracellular delay and virus clearance but varying half-life of infected cells are compared. However, even the most frequent samples available at the moment (9) cannot be used to assess the *smoothness* of the transition phase with sufficient precision to distinguish

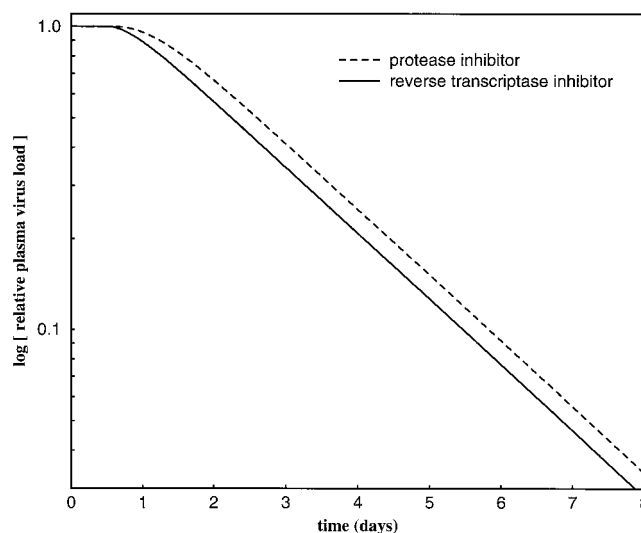


FIG. 2. Model predictions for plasma virus decline. Compared are solutions for reverse transcriptase inhibitors (Eq. 10) and protease inhibitors (Eq. 12). Parameter values that generate curves resembling clinical data are used, $a = 0.5/\text{day}$, $u = 3.0/\text{day}$, and $\tau = 12$ h.

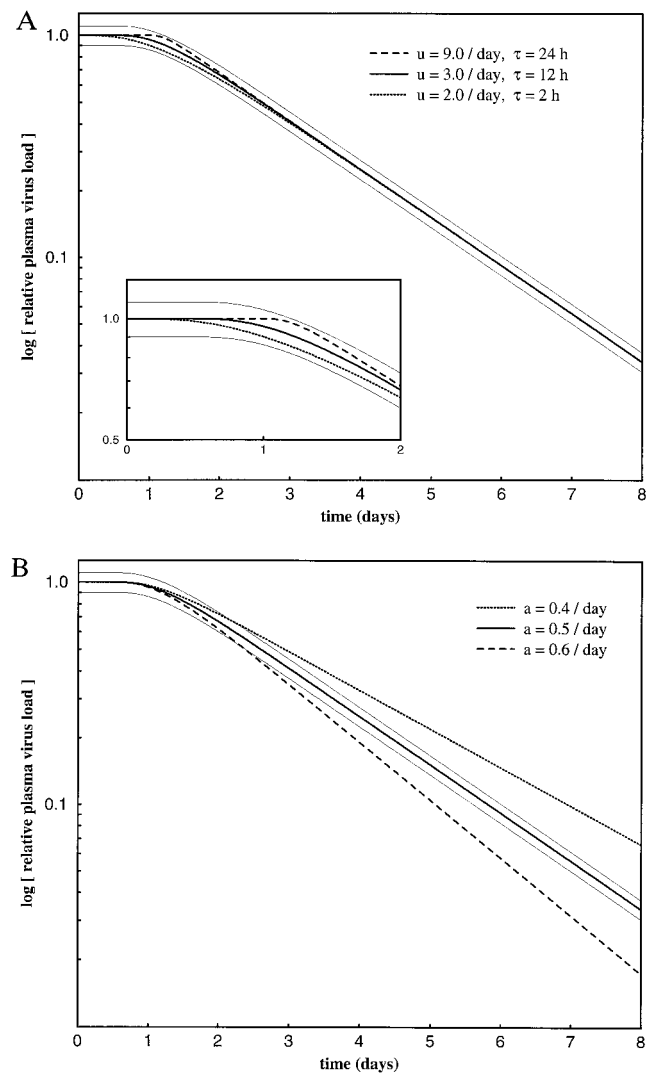


FIG. 3. Parameter sensitivity of the protease inhibitor model (Eq. 12). In *A*, the parameter a is fixed ($a = 0.5/\text{day}$) whereas u and τ vary; in *B*, u and τ are fixed ($u = 3.0/\text{day}$, $\tau = 12\text{ h}$) but a varies. The two thin lines represent 10% deviations from the mean solution to illustrate expected measurement errors under ideal experimental conditions; for the shoulder phase, fluctuations in current clinical measurements are of the order of 50% (1, 2, 9). As is clearly visible, clinical data do not provide enough information to distinguish between solutions in the first case but do so in the second case. The solutions in a were generated as follows. For $u > a$, the decline of free virus is $v(t) = v_0[u/(u-a)]^2 e^{-a(t-\tau)}$ in the limit $t \rightarrow \infty$. Taking logarithms on both sides gives $at + \ln[V(t)/V_0] = a\tau + 2 \ln[u/(u-a)]$. The right-hand side of the last equation does not depend on t . Thus all solutions with equal a and $C \equiv a\tau + 2 \ln[u/(u-a)]$ start with the same value at $t = 0$ and approach each other again for long times.

reliably between different solutions such as those shown in Fig. 3*A*. It follows that precise estimates of the pharmacological delay, the intracellular delay, and free virus half-life are impossible with current data on plasma virus decay.

The average viral generation time T in equilibrium is $T = \tau + u^{-1} + a^{-1}$. The formula holds for arbitrary $f(\tau) > 0$. (A derivation for the case $\tau = 0$ is given in ref. 9 and is readily extended to nonzero τ .) If, as in Fig. 3*A*, experimental uncertainties in u and τ are positively correlated, they partly cancel in the estimate for T . In this case the generation time can be determined with higher accuracy than u or τ . For example, if we use the three curves of Fig. 3*A* and assume that $\tau_{\text{pharm}} = 1\text{ h}$, the first and third solution correspond to intracellular delays of 1 and 23 h, respectively. The generation time T then varies by only roughly 20%, from $T = 2.5$ to $T = 3.1$ days.

Perelson *et al.* (9) used their differential equation model to calculate the free virus half-life to be around 0.24 day. For the data analysis, Perelson *et al.* implicitly took Eq. 12 but interpreted τ as a purely pharmacological delay, τ_{pharm} , which they constrained to be 2, 4, or 6 h. This situation differs conceptually from our approach. Here Eq. 12 follows from a dynamic description of the short-time HIV dynamics that explicitly incorporates intracellular delays. Within this framework, τ is replaced by $\tau \rightarrow \tau_{\text{pharm}} + \tau$ if clinical data are to be fitted, as explained in the previous section.

In their second, heuristic model, Perelson *et al.* (9) correctly attributed the length of the shoulder to the effect of pharmacological and intracellular delays, and the half-life of free virus and infected cells. However, their estimates for the intracellular delay τ and virus decay rate u are not consistent with each other. In their mathematical model, Perelson *et al.* assumed $\tau = 0$ and obtained $u = 3.1/\text{day}$. They then used this estimate for u in their heuristic approach to get $\tau = 0.9$ day.

Hepatitis B Dynamics

In the HBV life-cycle reverse transcriptase inhibitors block the production of new virus particles from infected cells. For drugs with high effectiveness the decline of HBV plasma virus load thus only reflects the decay of free virus (5), unlike the situation in HIV-1. There is some evidence that reverse transcriptase inhibitors also prevent the infection of uninfected cells (as in HIV-1), but because virus production is blocked this effect of the drug would not be visible in the virus decline data. Additional measurements such as hepatitis e antigen decline or resurgence of virus after cessation of therapy are therefore required to calculate the half-life of infected cells.

In chronic HBV infection, free virus has a half-life of about 1.0 day. Half-lives of productively infected cells seem to vary greatly among different patients, ranging from 10 to 100 days (5, 11). Interestingly, plasma virus clearance in patients treated with reverse transcriptase inhibitors is seemingly achieved in the absence of any antibodies to free virus particles. Furthermore, there is no indication of drug resistance even after more than 24 weeks of treatment.

In the context of the present model, treatment of HBV infection is represented by $k(t) = 0$ for $t > \tau_{\text{pharm}}$. Thus virus decline should be exponential following a time lag that only represents the pharmacological delay. This means that for HBV—in contrast with HIV—frequent and early sampling of plasma virus should provide good estimates of the pharmacological delay and confirm the estimate of free virus half-life. Currently available measurements of the virus load are, however, not yet frequent enough to exhibit the clear shoulder necessary for the calculation of the pharmacological delay.

Discussion

For drug treatment of HIV-1 with potent inhibitors of reverse transcriptase or protease, our model of short-time viral dynamics predicts that plasma virus decline starts after a time lag which is the sum of the pharmacological delay of the drug plus the intracellular delay of the viral life cycle. After a transition phase that depends on whether a reverse transcriptase inhibitor or a protease inhibitor has been administered, virus decline is roughly exponential. Long-term phenomena, such as the approach to a new quasi equilibrium are not an objective of the model.

For a treatment of HIV-1 with reverse transcriptase inhibitors or protease inhibitors, our specific conclusions are as follows. (i) The turnover rate of productively infected cells can be estimated with reasonable accuracy from the rapid decline of plasma virus (1, 2, 4). (ii) Plasma virus data do not allow a clear distinction between the effects of pharmacological delay,

intracellular delay, and the decay of free virus during the transition phase. Very different values for these parameters can lead to very similar time evolutions. (*iii*) The largest differences occur at roughly the maximal possible delay, in the present example between day 1 and 2. This implies that in order to improve the parameter estimates, frequent clinical measurements should continue at least until day 2.

The above conclusions are derived for a step-like onset of virus production after infection and a step-like onset of drug effectiveness. In reality, both virus production and drug effectiveness increase gradually. This makes decay curves smoother, provided other parameters remain unchanged. In other words, to fit *given* clinical data, the clearance of free virus has to be more rapid than in a model with step-like characteristics. This implies that both the present model and earlier approaches (1, 2, 9) systematically overestimate the true half-life of free virus. In (quasi-)equilibrium, virus clearance equals virus production. Virus production rates may therefore be significantly higher than predicted by previous models (1, 2, 9). On the other hand, the estimate for the half-life of infected cells is quite robust.

Improved models of the pharmacodynamics will play a major role in the assessment of the true decay rate of free virus. Thus a sensible and important extension of the current work is to include equations that capture drug absorption from the gut into the blood, and drug efficacy on the vital parameters controlling viral replication and cell infection. Additional independent measurements are necessary to achieve better parameter estimates. Pharmacological processes could be quantified based on measurements of drug concentration effects. In patients treated with protease inhibitor, measurements of the titer of infectious virus in plasma could be obtained to estimate the half-life of free-virus separately (9). Ideally, methods should be developed to quantify the amount of productively infected cells in various tissues.

For a treatment of HBV with a reverse transcriptase inhibitor, our specific conclusions are as follows. (*i*) We expect that there is an initial time lag, which is only caused by the pharmacological delay of the drug. The intracellular delay does not affect virus decline. (*ii*) If drug treatment effectively blocks the production of free virus, the decay of plasma virus is exponential and reflects the turnover of free virus particles (5). (*iii*) Frequent and early sampling of plasma HBV load should provide accurate estimates for the pharmacological delay and confirm the estimated clearance rate of free virus.

As shown in this article, simple mathematical models of virus–host cell interaction together with clinical data from drug-treated patients enable us to estimate important rate

constants of virus replication *in vivo*. The models also provide insight into current limitations of the data analysis and suggest specific new experiments to improve parameter estimates.

This approach combines experimental and theoretical methods and will extend our qualitative as well as quantitative understanding of short-term virus dynamics. In both HIV and HBV infections, however, the dynamics of disease progression occurs on a different time scale—years rather than days—and requires additional mathematical models that outline specific mechanisms of pathogenesis (12–15).

We would like to thank Beatrice Hahn, Alan Perelson, George Shaw, and Bernhard Sulzer for helpful discussions, and David Krakauer and Robert Payne for critical comments on the manuscript. This work was supported by the Commission of the European Communities (A.V.M.H.) and the Wellcome Trust (S.B., R.M.A., and M.A.N.).

1. Wei, X., Ghosh, S. K., Taylor, M. E., Johnson, V. A., Emini, E. A., Deutsch, P., Lifson, J. D., Bonhoeffer, S., Nowak, M. A., Hahn, B. H., Saag, M. S. & Shaw, G. M. (1995) *Nature (London)* **373**, 117–122.
2. Ho, D. D., Neumann, A. U., Perelson, A. S., Chen, W., Leonard, J. M. & Markowitz, M. (1995) *Nature (London)* **373**, 123–126.
3. Coffin, J. M. (1995) *Science* **267**, 483–489.
4. Nowak, M. A., Bonhoeffer, S., Loveday, C., Balfe, P., Semple, M., Kaye, S., Tenant-Flowers, M. & Tedder, R. (1995) *Nature (London)* **375**, 193.
5. Nowak, M. A., Bonhoeffer, S., Hill, A. M., Boehme, R., Thomas, H. C. & McDade, H. (1996) *Proc. Natl. Acad. Sci. USA* **93**, 4398–4402.
6. Larder, B. A., Darby, G. & Richman, D. D. (1989) *Science* **243**, 1731–1734.
7. McLean, A. R. & Nowak, M. A. (1992) *AIDS* **6**, 71–79.
8. Schuurman, R., Nijhuis, M., Vanleeuwen, R., Schipper, P., DeJong, D., Collis, P., Danner, S. A., Mulder, J., Loveday, C., Christopherson, C., Kwok, S., Sninsky, J. & Boucher, C. A. B. (1995) *J. Infect. Dis.* **171**, 1411–1419.
9. Perelson, A. S., Neumann, A. U., Markowitz, M., Leonard, J. M. & Ho, D. D. (1996) *Science* **271**, 1582–1586.
10. Winslow, D. L. & Otto, M. J. (1995) *AIDS* **9** (Suppl. A), S183–S189.
11. Marchuk, G. I., Petrov, R. V., Romanyukha, A. A. & Bocharov, G. A. (1991) *J. Theor. Biol.* **151**, 1–40.
12. Nowak, M. A., Anderson, R. M., McLean, A. R., Wolfs, T., Goudsmit, J. & May, R. M. (1991) *Science* **254**, 963–969.
13. Payne, R. J. H., Nowak, M. A. & Blumberg, B. S. (1994) *Math. Biosci.* **123**, 25–58.
14. McLean, A. R. & Nowak, M. A. (1992) *J. Theor. Biol.* **155**, 69–102.
15. Perelson, A. S., Kirschner, D. E. & DeBoer, R. (1993) *Math. Biosci.* **114**, 81–125.